



Fermi National Accelerator Laboratory
P.O. Box 500 • Batavia, Illinois • 60510

TD - 03 - 001
December 20, 2002

Nb₃Sn Shell-Type Mirror Magnet, HFDA-03A Production Report

**D. R. Chichili¹, G. Ambrosio², N. Andreev¹, E. Barzi²,
S. Bhashyam¹, L. Imbasciati, V. Kashikhin¹, V. Kashikhin²,
I. Novitski¹, S. Yadav¹, R. Yamada², and A.V. Zlobin²**

¹Engineering and Fabrication Department

²Development and Test Department

Technical Division

Fermilab, Batavia, IL 60510

1.0 Introduction

The mirror magnet, HFDA-03A has two main goals – to test the mechanics of the mirror magnet structure with bolted skin and to get an idea on the effect of eddy currents due to high inter-strand resistance on the quench performance of the magnet.

The half coil, HFDAH-05 from the magnet, HFDA-03 was selected to be used for this mirror magnet. Several modifications were done to this half-coil and the following section discusses these changes.

2.0 Changes to the Half-Coil

The fabrication of half coil, HFDAH-05 has been outlined in HFDA-03 production report¹. Four splices, two in the inner layer and two in outer layer were added in the mid-plane of the coil. These splice joints would increase the current sharing between the strands thus reducing the eddy current effect. Two splices per layer – one near the LE and the other near the RE - were joined. The splice joints at the LE for both the layers of the half-coil have a long lead, which could be used as power leads instead of the original ones. This would aid us in understanding whether the poor quench performance is due to cable degradation occurred during splicing or due to the proposed eddy current effects. Figs. 1 and 2 shows the half coil with the LE and RE splice joints respectively –



Fig. 1: Photograph showing the LE splice joints with long leads.

¹ TD-01-064, Nb₃Sn Cos (θ) Dipole Magnet, HFDA-03 Production Report

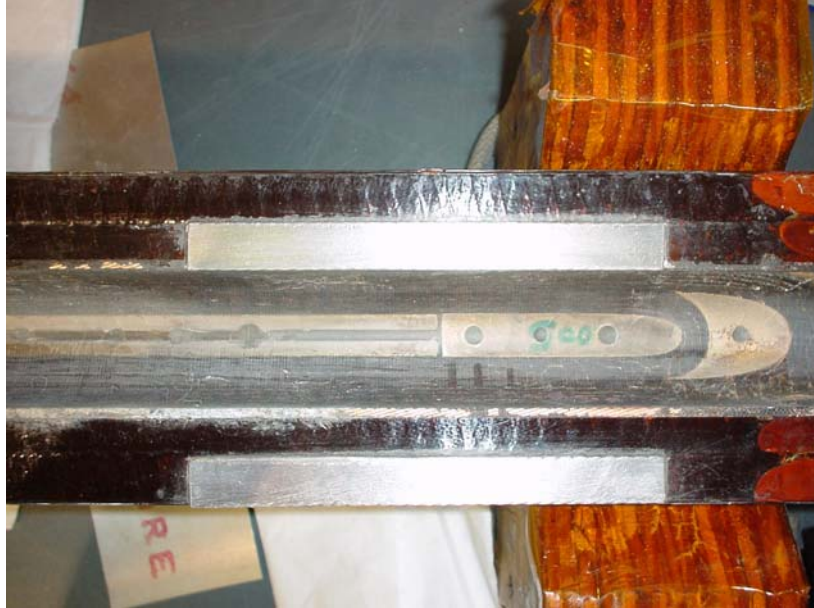


Fig. 2: *Photograph showing the RE splice joints*

The next step was to instrument the half coil. Fig. 3 shows the coil with instrumentation. Fig. 4 shows the voltage tap, temperature sensor and spot heater lay out. The rest of the mid-plane was filled with G-10 shims and were glued in place using the epoxy impregnation fixture. Fig. 5 shows the half coil after this operation.



Fig. 3: *Half coil with all the instrumentation*

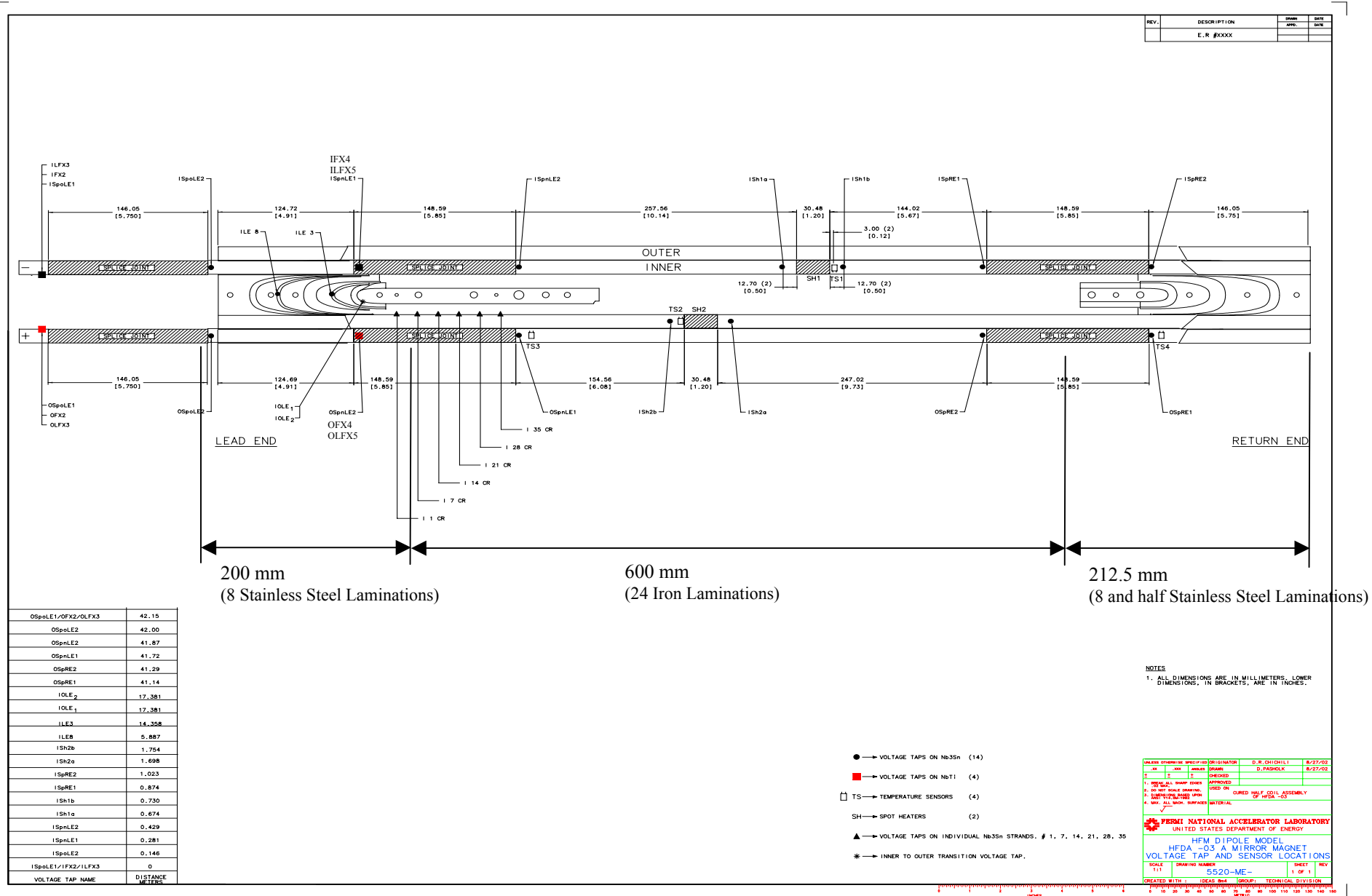


Fig. 4: Instrumentation layout



Fig. 5: *Mid-plane of the coil filled with G-10 shims and glued using impregnation fixture*

3.0 Instrumentation

The coil was instrumented with 4 temperature sensors (Cernox CX-1050-SD) and two spot heaters. Two temperature sensors, TS1 and TS2 were set very close to spot heaters SH1 and SH2 respectively. Together they will be used for local temperature margin measurements. This technique, introduced during the tests of HFDB-02 and described in TD-02-024, allows an estimation of the local critical current of the cable in case the current is limited by damage in another location.

One temperature sensor (TS3) was set close to the new LE splice in contact with the Nb₃Sn cable. This is the location where quenches originated in all previous tests of Cos-theta coils and this sensor should record any temperature increase due to heat coming from the splice. The splice on the outer layer was selected for this measurement because this splice is better thermally insulated, from the helium in the aperture, than the one on the inner layer. Another temperature sensor (TS4) was set close to the “dummy splice” on the RE. This sensor should record any temperature increase due to heat generated by the redistribution of BICCs (boundary induced coupling currents). The redistribution should occur mainly at the splices if the inter-strand resistance is high (possibly by an effect of the ceramic binder). Also this sensor was set on the outer layer for a better thermal insulation.

Several voltage taps were attached to measure the resistance of different splices and to locate the quench origin. Six voltage taps were also attached on single strands on the first turn of the inner layer. These six wires have been twisted together and the signals will be compared in an attempt to detect uneven current distributions in the cable due to BICCs. The voltage taps were set on the cable edge toward the aperture. There is a voltage tap every seven strands (i.e. strands 1, 7, 14, 21, 28 and 35).

4.0 Yoking/Clamping

Iron mirror was first placed on top of the half coil and then aluminum spacers were used to hold them together as shown in the Fig. 6. Two Kapton layers totaling 50 μm were placed on the radial surface of the half coil to create interference between the coil surface and the spacer. Kapton layers were also placed on the outer surface of the iron mirror such that there is a clearance of 0.1 mm between the spacer inner radius and the mirror outer radius. Note that the nominal ground insulation thickness on the iron mirror is 0.5 mm.



Fig. 6: *Half-coil with iron mirror and aluminum spacer*

The coil assembly was then placed in the yoke. Fig. 7 shows the coil in the yoke assembly. The layout of the iron yoke and stainless steel laminations with respect to the coil is shown in Fig. 4. There are 8 stainless steel laminations in the LE, 24 iron yoke in the straight section and 8 and half stainless steel laminations in RE per half magnet. Note that each lamination is 25 mm thick. The yoking/clamping procedure followed was similar to that of the previous dipole magnets. The spacers were instrumented with strain gauges to measure the azimuthal stress and two capacitance gauges were inserted in the outer layer pole region. The layout of the gauges is similar to that of HFDA-03. Figs. 8 and 9 show the evolution of azimuthal stress in the outer layer pole region and the spacer during yoking with and without the radial shim on the coil. Note that the radial shim was added to minimize the contribution of the pre-stress to the coil due to the skin during bolting operation. With the addition of the radial shim, there is more transfer of load to the coil thus reducing the stress in the spacers. During the entire operation, 50 mil shim was placed between the yoke halves in the LE and RE to prevent over-compression especially the lead cable and splice joints in LE.



Fig. 7: Coil + iron mirror in the yoke assembly

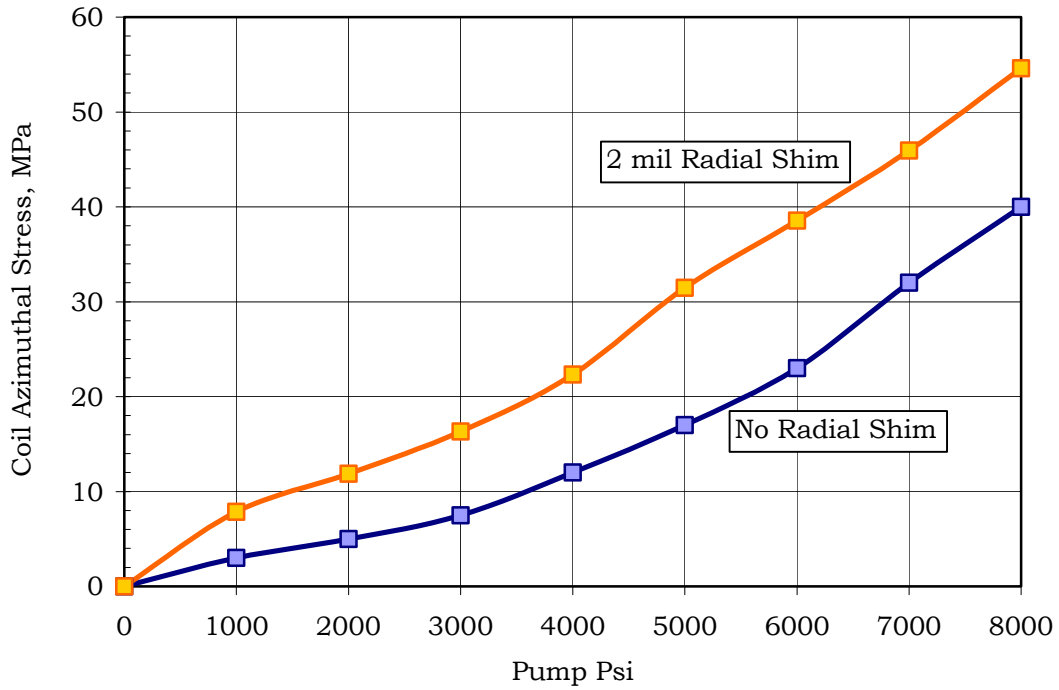


Fig. 8: Evolution of coil azimuthal stress during yoking operation

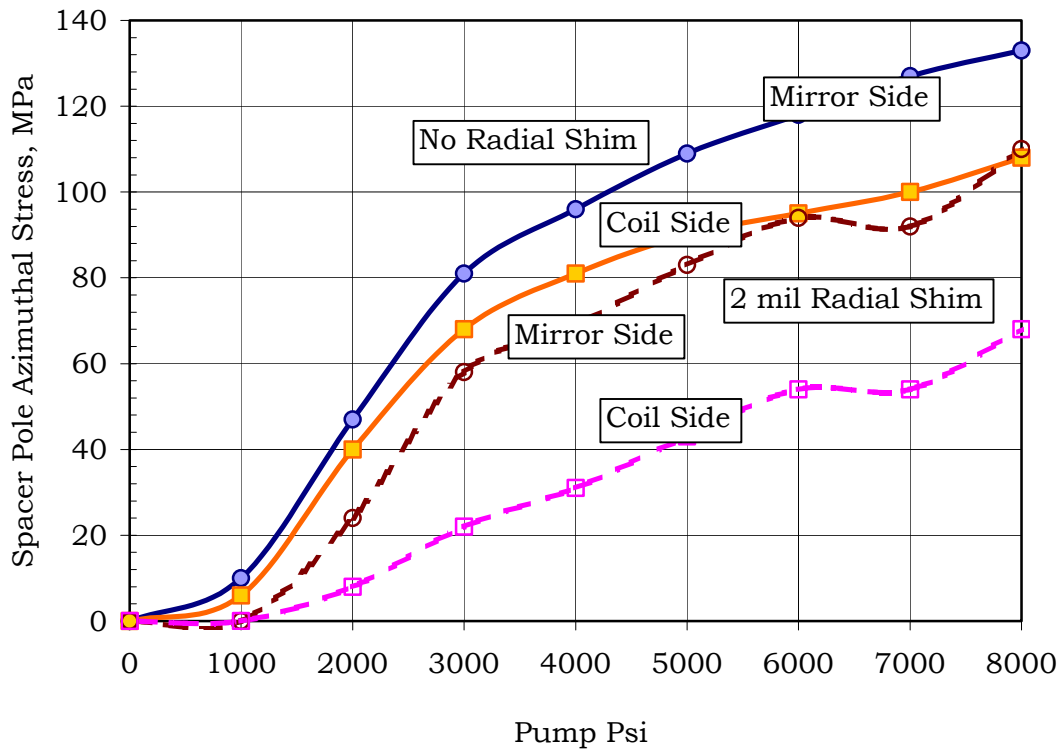


Fig. 9: Evolution of azimuthal stress in the spacer during yoking operation

At 8000 Pump Psi, the clamps were inserted using a separate set of pusher blocks. Two clamps one on each side were inserted simultaneously starting from the middle of the magnet. The coil resistance was monitored during the yoking/clamping operation to detect any possible coil to ground or heater to ground shorts. Table 1 shows the data along with ANSYS predictions. After spring back, the azimuthal stress in the coil is about 17 MPa compared to 25 MPa predicted by analysis.

	Under Press @ 8000 Pump Psi MPa	After Spring back MPa	After Skinning MPa
Coil Outer layer Pole Region	54 (45)*	17 (25)	28 (26)
Spacer Pole Region (Coil)	68 (90)	43 (50)	58 (119)
Spacer Pole Region (Mirror)	110 (105)	68 (58)	79 (110)
Spacer Mid-Plane Region	33 (35)	37 (33)	40 (86)

Table 1: Summary of data (azimuthal stress) collected during yoking and skinning operation. * The numbers in the brackets are ANSYS predictions with 0.05 mm interference between coil and spacer, 0.1 mm clearance between mirror and spacer and equivalent weld shrinkage of 0.1 mm.

5.0 Magnet Assembly

Skin halves were placed around the yoked assembly. Note that the bolted skin structure had to be formed into shape atleast for the first time since it was bend slightly out of shape due to the welding of the flanges. Smaller diameter bolts were first used to get the skin in shape and then they were successively replaced with the correct size bolts. Fig. 10 shows the coil with the bolted skin around.

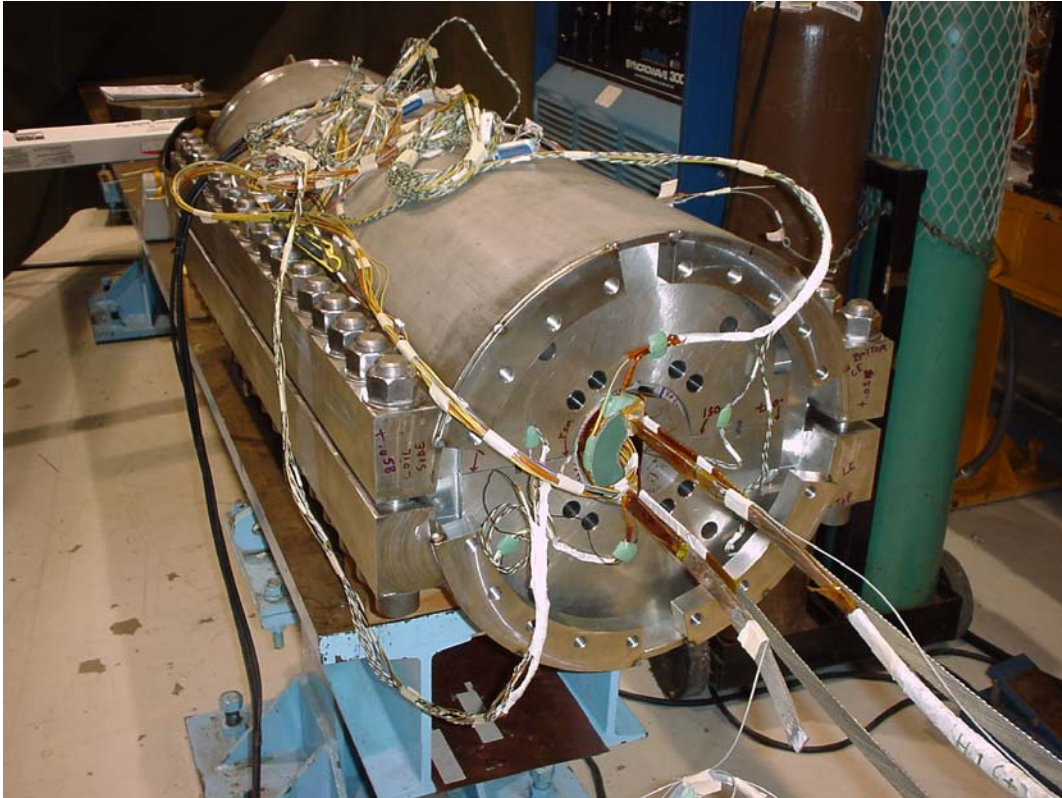


Fig. 10: *Mirror magnet with bolted skin*

The stress in the coil and in the spacers was monitored throughout the bolting process. The final stress values are given in Table 1. Note that the values for the stresses in the spacer do not match with that of the ANSYS calculations. One of the uncertainties is the spacer/pole interference, which determines the stress in the spacer. Since we created interference between the coil and the spacer by adding 50 μm of Kapton shim, this would reduce the spacer/pole interference. This in turn will reduce the stress in the spacer as more load is transferred to the coil. For more on ANSYS analysis see TD-02-047.

The next step was to install the end plates. For this the flanges were first welded to the bolted skin as shown in Fig. 10. The end plates were then bolted to these flanges and the final assembly is shown in Fig. 11. The lead cables coming out were secured in a G-10 plate before bending and routing them through the hole in the standoff plate as shown in Fig. 12.



Fig. 11: *Final assembly of the magnet.*

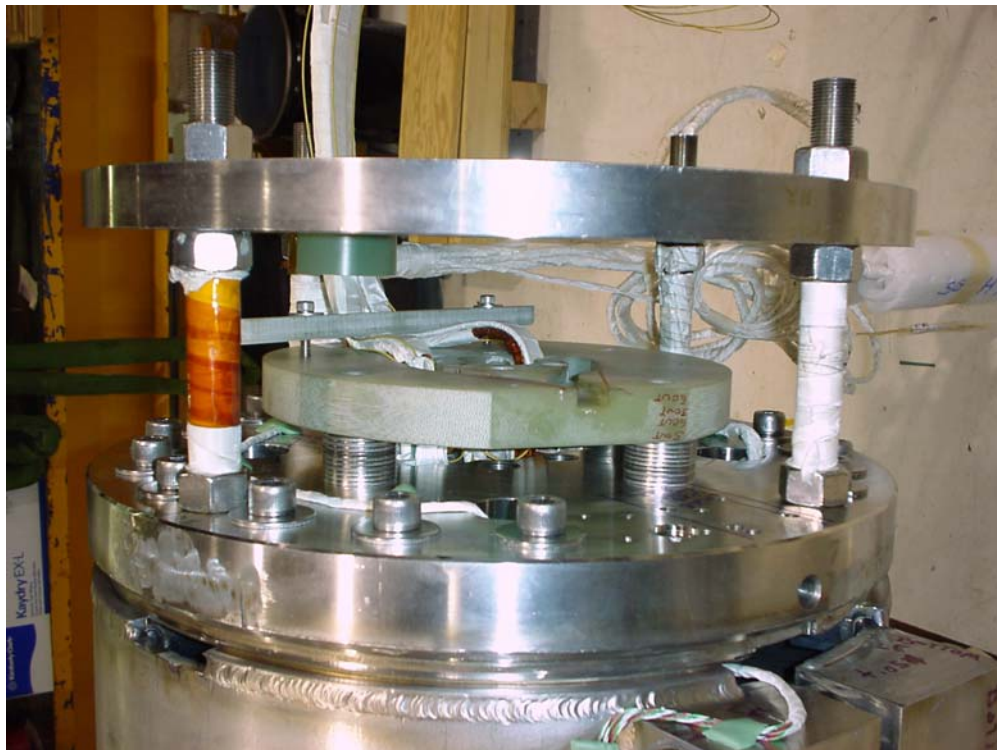


Fig. 12: *Close-up view of the power leads and standoff plate.*